

***In Situ* Signature of Cyclotron Resonant Heating in the Solar Wind**

Trevor A. Bowen<sup>1,\*</sup>, Benjamin D. G. Chandran<sup>2</sup>, Jonathan Squire<sup>3</sup>, Stuart D. Bale<sup>1,4</sup>, Die Duan<sup>5</sup>, Kristopher G. Klein<sup>6</sup>, Davin Larson<sup>1</sup>, Alfred Mallet<sup>1</sup>, Michael D. McManus<sup>1,4</sup>, Romain Meyrand<sup>3</sup>, Jaye L. Verniero<sup>7</sup>, and Lloyd D. Woodham<sup>8</sup>

<sup>1</sup>Space Sciences Laboratory, University of California, Berkeley, California 94720-7450, USA

<sup>2</sup>Department of Physics and Astronomy, University of New Hampshire, Durham, New Hampshire 03824, USA

<sup>3</sup>Department of Physics, University of Otago, 730 Cumberland Street, Dunedin 9016, New Zealand


<sup>4</sup>Physics Department, University of California, Berkeley, California 94720-7300, USA

<sup>5</sup>School of Earth and Space Sciences, Peking University, Beijing 100871, China

<sup>6</sup>Department of Planetary Sciences and Lunar and Planetary Laboratory, University of Arizona, Tucson, Arizona 85721, USA

<sup>7</sup>NASA Goddard Space Flight Center, 8800 Greenbelt Rd, Greenbelt, Maryland 20771, USA

<sup>8</sup>Department of Physics, The Blackett Laboratory, Imperial College London, London SW7 2AZ, United Kingdom

 (Received 9 November 2021; revised 20 June 2022; accepted 16 September 2022; published 14 October 2022)

The dissipation of magnetized turbulence is an important paradigm for describing heating and energy transfer in astrophysical environments such as the solar corona and wind; however, the specific collisionless processes behind dissipation and heating remain relatively unconstrained by measurements. Remote sensing observations have suggested the presence of strong temperature anisotropy in the solar corona consistent with cyclotron resonant heating. In the solar wind, *in situ* magnetic field measurements reveal the presence of cyclotron waves, while measured ion velocity distribution functions have hinted at the active presence of cyclotron resonance. Here, we present Parker Solar Probe observations that connect the presence of ion-cyclotron waves directly to signatures of resonant damping in observed proton-velocity distributions using the framework of quasilinear theory. We show that the quasilinear evolution of the observed distribution functions should absorb the observed cyclotron wave population with a heating rate of  $10^{-14}$  W/m<sup>3</sup>, indicating significant heating of the solar wind.

DOI: [10.1103/PhysRevLett.129.165101](https://doi.org/10.1103/PhysRevLett.129.165101)

**Introduction.**—Observations of the solar corona reveal plasma that is millions of degrees hotter than the blackbody temperature of the solar surface. While the energy required to heat the corona and accelerate the solar wind originates from solar convection and the magnetic fields produced by the solar dynamo, the specific pathways to heating and particle acceleration remain elusive [1]. The dissipation of Alfvénic turbulence at kinetic scales has become a common paradigm in explaining the dynamics of coronal heating and solar wind acceleration [2–5]; possible dissipative mechanisms include Landau or cyclotron resonant damping [6–10], stochastic heating [11], or magnetic reconnection [12,13]. Additionally, the portion of energy deposited by these processes at ion scales, versus that which is subject to a kinetic cascade and dissipated by electrons, remains an open question [10,14–17].

It is well known that the observed ion temperature profiles in the solar wind require significant perpendicular heating [18,19], which is likely initiated at ion kinetic scales where particles interact efficiently with electromagnetic waves [9,16,20–24]. Cyclotron resonant coupling of electromagnetic fluctuations with ion gyromotion [25] has received particular attention as a potential perpendicular heating mechanism [26–30]. Ultraviolet spectroscopic measurements of coronal ion temperature anisotropy

suggest large  $T_{\perp}/T_{\parallel}$ , consistent with cyclotron resonant heating [28,31–33]. The presence of ion-cyclotron waves has been well documented in *in situ* observations throughout the heliosphere both as solitary waves and as part of the background spectrum of fluctuations [34–40]. Observations of magnetic helicity at ion scales have been interpreted as evidence for active cyclotron damping of quasiparallel Alfvénic fluctuations, which contribute to turbulent heating [8,9,41,42].

Theoretical signatures of resonant interactions in particle distribution functions are often studied in the framework of quasilinear (QL) diffusion [15,43–45]; observations of the solar wind have suggested evidence for QL cyclotron resonant diffusion in signatures of the proton-velocity distribution function  $f_p(\mathbf{v})$  [46–48]. While the generation of cyclotron waves through instabilities has been widely discussed [37,38,40,49,50] and signatures of cyclotron resonant dissipation have been suggested [8,9,46,48,51–53], definitive cyclotron resonant heating sufficient to power the solar wind has not been observed.

In this Letter, we apply the QL theory of resonant cyclotron interactions [43,44] to empirically measured cyclotron wave spectra and ion-distribution functions. Our results provide evidence of substantial heating at levels comparable with bulk solar wind heating rates,

providing a compelling picture of ion heating in the solar wind.

*Data.*—Parker Solar Probe (PSP) [54] observations from the electromagnetic FIELDS [55] and Solar Wind Electron Alpha and Proton (SWEAP) [56] instruments aim to constrain fundamental processes that result in coronal heating and solar wind acceleration. PSP has revealed prevalent ion-scale electromagnetic waves [39,40], ion distributions out of thermal equilibrium [57,58], and evidence for resonant wave-particle interactions predicted by QL theory [59]. To constrain cyclotron resonant heating, we study a stream from PSP perihelion 4 on January 30, 2020 from 00:00–08:00 hrs with resolved proton distributions. During the interval, PSP was  $\sim 30R_\odot$  from the solar surface. We use merged search coil and fluxgate magnetometer data from PSP FIELDS [55,60] enabling measurement of the inertial, transition, and kinetic scales of turbulence; the merged dataset only has two axes available [61], thus we use vector-fluxgate magnetometer data to study wave polarization. Figure 1(a) shows  $\mathbf{B}$  in radial-tangential-normal (RTN) coordinates. Proton-velocity distribution functions  $f_p(\mathbf{v})$  are obtained from the PSP SWEAP Solar Probe ANalyzer (SPANi). The proton population is often parametrized with a pair of drifting bi-Maxwellian fits to model  $f_p(\mathbf{v})$  using separate thermal (core) and nonthermal (beam) populations [1]. Fits to a proton core and field-aligned beam provide estimates of

bulk velocity  $\mathbf{u}$ , anisotropic temperatures perpendicular and parallel to the background magnetic field  $T_{\perp,\parallel}$ , and the beam-to-core proton density ratio  $n_b/n_c$  [56,58]. Figure 1(b) shows measurements of  $\mathbf{u}$  in RTN coordinates. The stream is relatively slow with an average speed of  $\sim 220$  km/s and moderately Alfvénic with a cross helicity of  $\sim 0.85$ .

The phase-space density of  $f_p(\mathbf{v})$  is calibrated to quasithermal noise (QTN) from FIELDS to recover the absolute density [55,62]. The mean proton density is  $n_p = 1100/\text{cm}^3$ ; SPANi gives an average beam-to-core density ratio of 0.48. The core has  $T_\perp$  of 15 eV and  $T_\parallel$  of 12 eV; the beam has  $T_\perp$  of 22 eV and  $T_\parallel$  of 30 eV. The average drift of the beam relative to the core is 83 km/s. The individual core and beam have  $\beta_c = 0.65$  and  $\beta_b = 1.1$ . The mean magnetic field was directed Sunward, with an Alfvén speed of 60 km/s. Figure 1(c) shows the magnetic field spectra of the interval with a steep transition range at ion-kinetic scales [63–65].

We apply a Morlet wavelet transform to the vector magnetic field data rotated into field-aligned coordinates [66]. Signatures of circular polarization are found using

$$\sigma_B(f, t) = -2\text{Im}(B_{\perp 1} B_{\perp 2}^*) / (B_{\perp 1}^2 + B_{\perp 2}^2), \quad (1)$$

with left- and right-handed waves corresponding to positive and negative  $\sigma_B$  [35,36,67,68]. Circular polarization is measured in the spacecraft frame, such that the measured sign may not correspond to the innate plasma frame polarization [67]. A sign change in  $\sigma_B$  occurs if the wave is Doppler shifted to negative frequencies in the spacecraft frame. However, it has been demonstrated that the majority of waves propagate outward, and thus, that Doppler shift does not change their handedness when observed in the spacecraft frame [69].

Previous work has shown that circularly polarized ion-scale waves are parallel propagating and evident when  $\theta_{vB} \sim 0$  [40]. However, observations of parallel-propagating, circular polarized waves are strongly inhibited when the angle between the solar wind and the mean magnetic field is oblique. This effect occurs because (a) the wave polarization plane is not well resolved by the spacecraft and (b) the turbulence is anisotropic with increasing power with larger  $\theta_{vB}$  [67,70–72]. The lack of circular polarization signatures when  $\theta_{vB}$  is moderately oblique is consistent with sampling effects of quasiparallel waves at oblique angles in anisotropic turbulence [40], suggesting that ion-scale waves can persist at oblique  $\theta_{vB}$ . In order to estimate the parallel-propagating, left-hand polarized spectrum, wavelet power with  $\sigma_B > 0.9$  is identified when  $\theta_{vB} < 15^\circ$ . We assume homogeneity and stationarity, such that the circularly polarized spectrum measured at  $\theta_{vB} < 15^\circ$  represents the wave spectrum at all times (i.e., when  $\theta_{vB} > 15^\circ$ ). Figure 1(c) shows the power spectrum of circularly polarized fluctuations with  $\sigma_B > 0.9$  and  $\sigma_B < -0.9$ , corresponding to strong left- and right-handed power. The right-handed modes have been

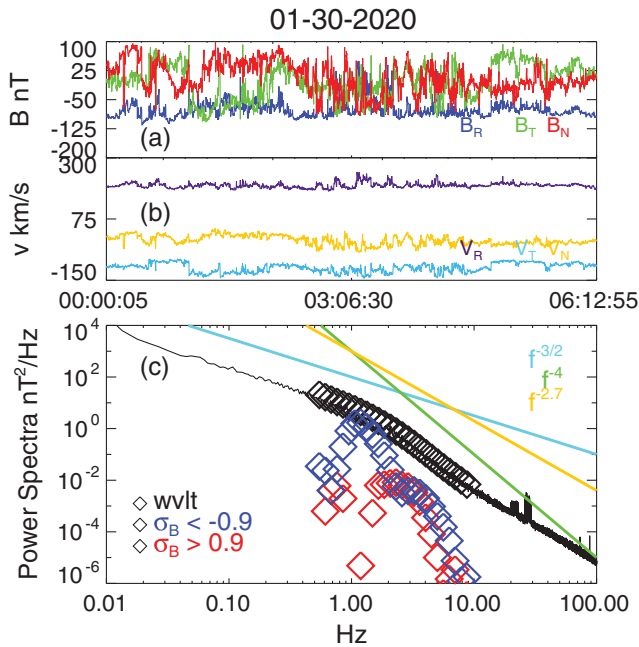


FIG. 1. (a) Magnetic field measurements from PSP-FIELDS. (b) Velocity measurements from PSP-SPANi. (c) Spectra of magnetic field data. Spectral indices at  $-3/2$ ,  $-4$  and  $-2.7$  are shown. Wavelet coefficients for total power are shown as black  $\diamond$ . Wavelet coefficients filtered by left- and right-handed  $\sigma_b$  are shown in red and blue  $\diamond$ .

shown to be statistically consistent with a fast magnetosonic mode [69].

*Distribution functions.*—Figure 2 shows the SPANi proton distribution function  $f_p(v_\perp, v_\parallel)$  from the stream at January 30, 2020 04:10:21 hrs. Figure 2(a) shows an interpolation of the 3D measurements in the  $v_\perp$ – $v_\parallel$  plane constructed by identifying values of  $v_\perp$  and  $v_\parallel$  for each 3D energy bin, assuming gyrotropy. A drifting two-component bi-Maxwellian fit, assuming gyrotropy, is shown in Fig. 2(b). The drifting bi-Maxwellian fit provides an approximation to  $f_p(\mathbf{v})$  using two individual proton populations, though this parametrization may not resolve all nonthermal features that affect resonant interaction with

cyclotron waves. Indeed, the presence of strong and persistent cyclotron resonant interactions should affect the shape of  $f_p(\mathbf{v})$ , leading to an equilibrium distribution that deviates from a bi-Maxwellian [44]. To explore a nonparametric  $f_p(v_\perp, v_\parallel)$ , which may better represent the data [73–75], we fit a set of orthonormal Hermite functions using linear least-square methods,

$$f_p(v_\perp, v_\parallel) = \sum_{m,n} g_{mn} \phi_m(v_\perp/v_{\perp\text{th}}) \phi_n(v_\parallel/v_{\parallel\text{th}}), \quad (2)$$

$$H_n(v) = (-1)^n e^{v^2} \frac{d^n}{dx^n} e^{-v^2}, \quad (3)$$

$$\phi_m = \frac{H_m(v)}{\sqrt{2^m \pi^{1/2} m!}} e^{-v^2} \quad (4)$$

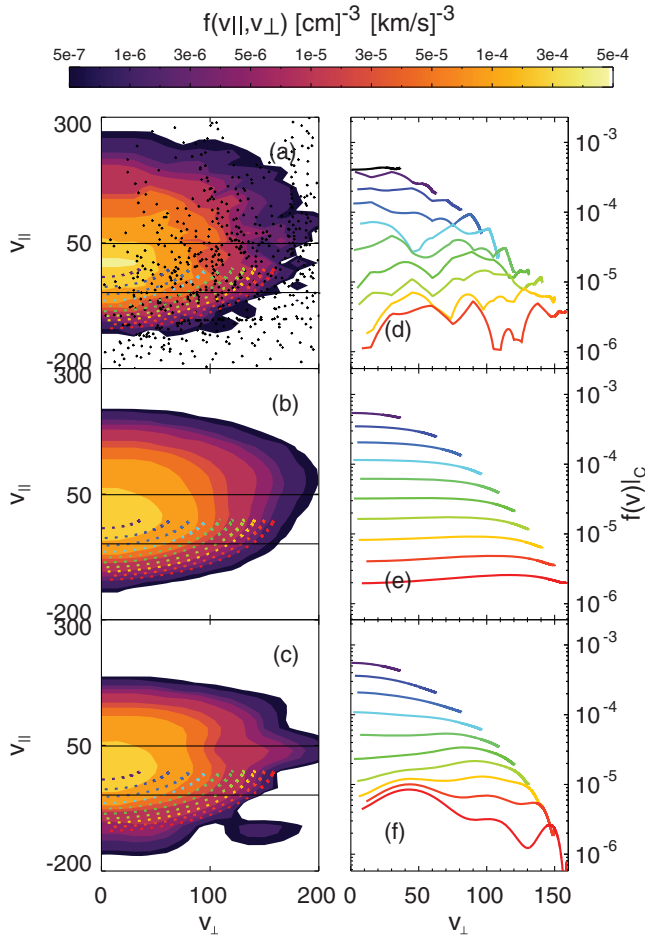


FIG. 2. (a) Interpolation of  $f_p(\mathbf{v})$  from SPANi in the  $v_\perp$ – $v_\parallel$  plane, with the mean magnetic field pointing vertically. Points show SPANi measurement locations. Solid lines show  $v_{\parallel\text{th}}$ , and a set of cyclotron resonant diffusion contours are plotted. (b) Drifting bi-Maxwellian fit to  $f_p(\mathbf{v})$ . (c) Hermite representation of  $f_p(\mathbf{v})$ . Integration of  $f_p(\mathbf{v})$  in (a)–(c) over  $v_\perp$ – $v_\parallel$  is normalized to the QTN density. (d) Contours of  $f_p(\mathbf{v})$  determined by interpolating the gyrotropic distribution along QL diffusion contours for parallel cyclotron resonance. (e),(f) Drifting bi-Maxwellian and the Hermite representations of  $f_p(\mathbf{v})$  evaluated along cyclotron resonance contours.

[76,77]. Figure 2(c) shows the best-fit estimate to  $f_p(\mathbf{v})$  for Hermite functions of order  $m_{\text{max}} = 6$  and  $n_{\text{max}} = 6$ . The distributions are shown in field-aligned coordinates with  $\hat{\mathbf{B}}_0$  along the vertical axis. In carrying out this fit, we effectively extend  $f(v_\perp, v_\parallel)$  to negative values of  $v_\perp$  by treating  $f(v_\perp, v_\parallel)$  as an even function of  $v_\perp$ , thereby omitting the terms in the sum corresponding to odd values of  $m$ . Our use of Hermite functions is meant solely as a nonparametric interpolative scheme and is not intended to represent a natural basis for  $f_p(\mathbf{v})$  [76]. Over the studied interval, the average  $\chi^2$  residual of the Hermite representation is 90% of the bi-Maxwellian fit. No intervals were significantly better fit by the drifting bi-Maxwellian, though some distributions are equally well represented by either approximation.

The ion-cyclotron resonance condition is  $\omega(k_\parallel) = \Omega + k_\parallel v_\parallel$  such that outward-propagating cyclotron waves resonate with the inward-propagating portion of the distribution function. The evolution of  $f_p(\mathbf{v})$  in the presence of resonant interactions can be described by QL diffusion theory [43,44]. In a reference frame moving with a wave, the particles conserve kinetic energy as they scatter off that wave, tracing contours in  $v_\perp$  and  $v_\parallel$  that can be computed using the wave dispersion relation and resonance condition [29,43,44,46]. The QL diffusion contours [44,78] are overlaid on  $f_p(\mathbf{v})$  in Figs. 2(a)–2(c). If  $f_p(\mathbf{v})$  decreases as  $v_\perp$  increases along the contours, cyclotron resonance diffuses energy across in the region where resonant waves are present, heating the plasma. Conversely, if  $f_p(\mathbf{v})$  increases as  $v_\perp$  increases, then  $f_p(\mathbf{v})$  is unstable, generating waves and cooling the plasma. Cyclotron resonant equilibrium corresponds to a flattening of  $f_p(\mathbf{v})$  along the contours. Figures 2(d)–2(f) show  $f_p(\mathbf{v})$  evaluated along QL diffusion contours, parametrized on  $v_\perp$ ; for each representation,  $f_p(\mathbf{v})$  is characteristically flat along contours, suggesting that  $f_p(\mathbf{v})$  has been processed by cyclotron resonance [46,48].

The QL proton heating rate due to resonance with parallel-propagating cyclotron waves is given by

$$\begin{aligned} \mathcal{H} &= \int \frac{m_p v^2}{2} \frac{\partial f_p(\mathbf{v})}{\partial t} d^3\mathbf{v} \\ &= \frac{\pi e^2}{2m_p^2} \int_0^\infty dk_{\parallel} \frac{1}{v_{\perp}} \hat{G}_k [v_{\perp} \delta(\omega_k - k_{\parallel} v_{\parallel} - \Omega_p) \\ &\quad \times \frac{\omega_k^2}{k_{\parallel}^2 c^2} I(k_{\parallel}) \hat{G}_k f_p(\mathbf{v})] d^3\mathbf{v} \end{aligned} \quad (5)$$

with

$$\hat{G}_k = \left(1 - \frac{k_{\parallel} v_{\parallel}}{\omega}\right) \frac{\partial}{\partial v_{\perp}} + \frac{k_{\parallel} v_{\perp}}{\omega} \frac{\partial}{\partial v_{\parallel}} \quad (6)$$

[43]. Using the observed left-handed spectrum in Fig. 1, the cold-plasma dispersion relation, along with the bulk velocity to correct for Doppler shift [69], an average parallel left-handed cyclotron spectrum  $I(k_{\parallel})$  is established.

For each observed  $f_p(\mathbf{v})$ , a value of  $\mathcal{H}$  is obtained numerically through Eq. (5) using bi-Maxwellian and Hermite representations of  $f(v_{\perp}, v_{\parallel})$ . For the distribution shown in Fig. 2, a heating rate of  $10^{-14}$  W/m<sup>3</sup> is found using the Hermite representation and  $4 \times 10^{-15}$  W/m<sup>3</sup> using the drifting bi-Maxwellian spectrum. The measured  $\mathcal{H}$  is similar to estimates of bulk ion heating due to turbulent dissipation at the spacecraft’s location ( $30R_{\odot}$ ) [79–81].

Figures 3(a)–3(d) show the differential volumetric heating rate  $\mathcal{H}$  as a function of resonant parallel velocity measured in each distribution function. The top panels, Figs. 3(a) and 3(b), show positive  $\mathcal{H}$ , the “heating” rate, as a function of  $v_{\parallel}$  and time for the (a) bi-Maxwellian and (b) Hermite representations. The bottom panels, Figs. 3(c) and 3(d), show negative  $\mathcal{H}$ , the “cooling” rate over the interval as a function of resonant  $v_{\parallel}$  due to emission of waves through instability. Figure 3(e) shows the net integrated  $\mathcal{H}$  for each measured distribution function. The integrated  $\mathcal{H}$  is uniformly positive, indicating that cyclotron waves present in the plasma are likely absorbed. There is very little cyclotron resonant emission from this plasma. However, the Hermite representation shows that cyclotron instability, when present, is focused at the parallel thermal speed,  $v_{\parallel\text{th}}$ . The median heating rate is  $3 \times 10^{-15}$  W/m<sup>3</sup> for the bi-Maxwellian fits and  $1 \times 10^{-14}$  W/m<sup>3</sup> for the Hermite representation. Using third-order moments of the inertial range turbulence [82], a cascade rate of  $4.7 \times 10^{-14}$  W/m<sup>3</sup> is measured, which is consistent with previous measurements of the energy cascade rate at a similar radius [83,84]. The measured cyclotron heating  $\mathcal{H}$  ranges from approximately 10%–20% of the measured cascade rate. While uncertainties on the cascade rate exist due to the assumption of stationarity,

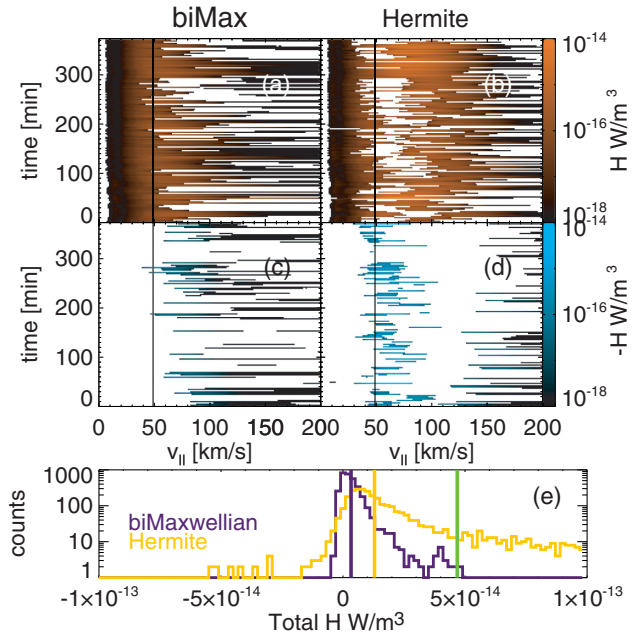


FIG. 3. (a) Differential volumetric heating rates (positive  $\mathcal{H}$ ) as a function of resonant parallel velocity computed from observed cyclotron spectra and drifting bi-Maxwellian fit to ion-distribution functions. The total heating rate is the sum over  $v_{\parallel}$ . Solid lines show the average  $v_{\parallel\text{th}}$  for the interval (49 km/s). (b) Measured heating rates for a Hermite function approximation. (c),(d) Corresponding cooling rates (negative  $\mathcal{H}$ ). (e) Distribution of total  $\mathcal{H}$  for bi-Maxwellian and Hermite representations; respective lines show median value of  $\mathcal{H}$ . The turbulent cascade rate estimated from third-order moments is shown in green.

isotropy, and homogeneity [82], previous work has suggested that the cascade rate estimates through third-order moments are accurate to a factor of approximately 2 or 3 [83,85,86].

Observations from SPANi are partial measurements of  $f_p(\mathbf{v})$  and are subject to both uncertainties and ongoing calibration work. However, during this interval,  $f_p(\mathbf{v})$  is well resolved, and while uncertainties in  $f_p(\mathbf{v})$  will dominate uncertainties in our measured heating rates, we argue that the measurements reliably suggest net energy transfer from waves to the particles. Specifically, the bi-Maxwellian fit removes fine structure in  $f_p(\mathbf{v})$  that is present in the measurements and replicated by the Hermite function; importantly, we find that removing fine structure (i.e., the bi-Maxwellian fit) produces heating rates of the same sign and order of magnitude as when fine structure in  $f_p(\mathbf{v})$  is included. In essence, while fine structure in  $f_p(\mathbf{v})$  is observed by SPANi, it neither drastically affects the order of magnitude, nor, importantly, the sign of the cyclotron heating rate  $\mathcal{H}$ . However, these results highlight the importance of modeling fine structure and local gradients in  $f_p(\mathbf{v})$ , e.g., with Hermite functions, which may yield heating rates more than double those found by smoother approximations to  $f_p(\mathbf{v})$ , e.g., a bi-Maxwellian fit.

*Discussion.*—Cyclotron resonance may play a significant role in shaping observed magnetic field spectra and distribution functions [8,9,23,42,46,48,52] observed in the solar wind. While flattening along QL diffusion contours has been previously reported [46,48,59], our observations directly couple an observed spectrum of cyclotron waves to heating rates in measured distribution functions. Our measured heating rates are on the order of the measured energy cascade rates ( $\sim 10^{-14}$  W/m<sup>3</sup>), obtained through third-order moments of the observed turbulence [82]; while this estimate may have significant uncertainty, we find good agreement with previous estimates of the cascade rate [83,84]. We furthermore show that incorporating fine, nonthermal structures in the distribution function using a Hermite functional decomposition introduces relatively little effect on the extent or sign of measured cyclotron heating. We thus argue that the measured levels of cyclotron heating provide significant evidence for the mediation of turbulent dissipation through cyclotron resonance that is potentially sufficient to power the solar wind [79–81]. Studying the radial scaling of the turbulent energy cascade alongside quasilinear cyclotron heating rates promises to further constrain cyclotron resonance as a dissipation process.

There are several sources of uncertainty in this analysis, rising predominantly in the estimate of the cascade rate and in the gradients of  $f_p(\mathbf{v})$  due to limited resolution. Furthermore, if the occurrence rates of cyclotron waves decreases with  $\theta_{vB}$ , then the heating rate may be limited at oblique  $\theta_{vB}$ . Additionally, there is the potential that heating by oblique kinetic Alfvén waves or oblique cyclotron waves may generate parallel cyclotron waves as a secondary process [87,88]. The spectrum of oblique cyclotron waves is difficult to distinguish due to the strong anisotropy of the background turbulence [40], though future work will explore signatures of oblique cyclotron resonance. In any case, observed ion distributions are often flat along the quasiparallel cyclotron diffusion contours and are rarely unstable to the growth of the waves. This flattening suggests that even if other physical processes contribute to bulk heating, the parallel cyclotron resonance [43,44] plays a significant role in shaping the distribution functions.

The measured heating rate indicates a near total lack of cyclotron emission through instabilities; thus, the origin of cyclotron waves remains an important unresolved point. Our observations show that 95% of the time that left-handed signatures are present, the net heating rate is positive, suggesting absorption of waves [53]. We note the studied interval does not have strong cyclotron wave storms [40,57], though application of our method to a similar interval with more significant cyclotron wave events similarly suggests net heating. There are two main possible physical origins for these Alfvén-ion-cyclotron waves. First, it is possible they are excited by beam instabilities [89], though recent work has suggested that dominant

instability associated with the strong beam is associated with right-handed modes [57,58]. Second, they may be generated by turbulence, though canonical theories of Alfvénic nonlinearity preferentially transport energy to large  $k_{\perp}$ , but not large  $k_{\parallel}$  [90,91], which is a hurdle to the turbulent generation of cyclotron resonant waves. However, recent work suggests that imbalance, i.e., the dominance of the outward Alfvén mode, may prevent energy from cascading to kinetic scales [92]. Fully kinetic simulations in the presence of such a barrier [88] show the generation of quasiparallel cyclotron modes, similar to those observed in the solar wind, providing a novel method for generating cyclotron waves that is consistent with a variety of observations [39,40,65,93–98]. Further work is required to specifically investigate the origin of the observed cyclotron waves and their connection to turbulence, though our observation of localized instability at the proton-core thermal speed (Fig. 3) may be a clue regarding the origin of the waves and their connection to the net heating measured in this study.

This Letter explicitly shows that the measured distribution functions in the solar wind contain evidence of cyclotron resonant heating at a level that may power the expanding solar wind. These results are significant step toward understanding the underlying physics of collisionless heating and a kinetic description of astrophysical plasmas.

T. A. B. thanks A. Chasapis, S. Servidio, and T. Dudok de Wit for their constructive input to this work. T. A. B. was supported by NASA PSP-GI Grant No. 80NSSC21K1771. K. G. K. was supported by NASA ECIP Grant No. 80NSSC19K0912. B. D. G. C. was supported in part by NASA Grant No. 80NSSC19K0829. J. L. V. was supported by NASA Grant No. NNH20ZDA001N-PSPGI. L. D. W. was supported by STFC consolidated Grant No. ST/S000364/1. D. D. acknowledges NSFC Grant No. 42204166. The authors additionally acknowledge PSP-SWEAP and FIELDS Contract No. NNN06AA01C.

\*tbowen@berkeley.edu

- [1] Eckart Marsch, Kinetic physics of the solar corona and solar wind, *Living Rev. Solar Phys.* **3**, 1 (2006).
- [2] Paul J. Coleman, Jr., Turbulence, viscosity, and dissipation in the solar-wind plasma, *Astrophys. J.* **153**, 371 (1968).
- [3] W. H. Matthaeus and M. L. Goldstein, Measurement of the rugged invariants of magnetohydrodynamic turbulence in the solar wind, *J. Geophys. Res.* **87**, 6011 (1982).
- [4] S. R. Cranmer and A. A. van Ballegooijen, Alfvénic turbulence in the extended solar corona: Kinetic effects and proton heating, *Astrophys. J.* **594**, 573 (2003).
- [5] Benjamin D. G. Chandran, Bo Li, Barrett N. Rogers, Eliot Quataert, and Kai Germaschewski, Perpendicular ion heating by low-frequency Alfvén-wave turbulence in the solar wind, *Astrophys. J.* **720**, 503 (2010).

- [6] A. Barnes, Collisionless damping of hydromagnetic waves, *Phys. Fluids* **9**, 1483 (1966).
- [7] A. Barnes, Hydromagnetic waves and turbulence in the solar wind, in *Solar System Plasma Physics*, edited by C. F. Kennel, L. J. Lanzerotti, and E. N. Parker (North-Holland, Amsterdam, 1979), Vol. 1, pp. 249–319.
- [8] M. L. Goldstein, D. A. Roberts, and C. A. Fitch, Properties of the fluctuating magnetic helicity in the inertial and dissipation ranges of solar wind turbulence, *J. Geophys. Res.* **99**, 11519 (1994).
- [9] Robert J. Leamon, William H. Matthaeus, Charles W. Smith, and Hung K. Wong, Contribution of cyclotron-resonant damping to kinetic dissipation of interplanetary turbulence, *Astrophys. J. Lett.* **507**, L181 (1998).
- [10] G. G. Howes, J. M. Tenborge, W. Dorland, E. Quataert, A. A. Schekochihin, R. Numata, and T. Tatsuno, Gyrokinetic Simulations of Solar Wind Turbulence from Ion to Electron Scales, *Phys. Rev. Lett.* **107**, 035004 (2011).
- [11] B. D. G. Chandran, D. Verscharen, E. Quataert, J. C. Kasper, P. A. Isenberg, and S. Bourouaine, Stochastic heating, differential flow, and the alpha-to-proton temperature ratio in the solar wind, *Astrophys. J.* **776**, 45 (2013).
- [12] Alfred Mallet, Alexander A. Schekochihin, and Benjamin D. G. Chandran, Disruption of Alfvénic turbulence by magnetic reconnection in a collisionless plasma, *J. Plasma Phys.* **83**, 905830609 (2017).
- [13] Nuno F. Loureiro and Stanislav Boldyrev, Role of Magnetic Reconnection in Magnetohydrodynamic Turbulence, *Phys. Rev. Lett.* **118**, 245101 (2017).
- [14] Eliot Quataert and Andrei Gruzinov, Turbulence and particle heating in advection-dominated accretion flows, *Astrophys. J.* **520**, 248 (1999).
- [15] Benjamin D. G. Chandran, Peera Pongkitiwanchakul, Philip A. Isenberg, Martin A. Lee, Sergei A. Markovskii, Joseph V. Hollweg, and Bernard J. Vasquez, Resonant interactions between protons and oblique Alfvén/ion-cyclotron waves in the solar corona and solar flares, *Astrophys. J.* **722**, 710 (2010).
- [16] Benjamin D. G. Chandran, Timothy J. Dennis, Eliot Quataert, and Stuart D. Bale, Incorporating kinetic physics into a two-fluid solar-wind model with temperature anisotropy and low-frequency Alfvén-wave turbulence, *Astrophys. J.* **743**, 197 (2011).
- [17] O. Alexandrova, C. Lacombe, A. Mangeney, R. Grappin, and M. Maksimovic, Solar wind turbulent spectrum at plasma kinetic scales, *Astrophys. J.* **760**, 121 (2012).
- [18] John D. Richardson, Karolen I. Paularena, Alan J. Lazarus, and John W. Belcher, Radial evolution of the solar wind from IMP 8 to Voyager 2, *Geophys. Res. Lett.* **22**, 325 (1995).
- [19] Lorenzo Matteini, Simone Landi, Petr Hellinger, Filippo Pantellini, Milan Maksimovic, Marco Velli, Bruce E. Goldstein, and Eckart Marsch, Evolution of the solar wind proton temperature anisotropy from 0.3 to 2.5 AU, *Geophys. Res. Lett.* **34**, L20105 (2007).
- [20] Eliot Quataert, Particle heating by Alfvénic turbulence in hot accretion flows, *Astrophys. J.* **500**, 978 (1998).
- [21] Robert J. Leamon, Charles W. Smith, Norman F. Ness, William H. Matthaeus, and Hung K. Wong, Observational constraints on the dynamics of the interplanetary magnetic field dissipation range, *J. Geophys. Res.* **103**, 4775 (1998).
- [22] S. Peter Gary, Collisionless dissipation wavenumber: Linear theory, *J. Geophys. Res.* **104**, 6759 (1999).
- [23] R. J. Leamon, W. H. Matthaeus, C. W. Smith, G. P. Zank, D. J. Mullan, and S. Oughton, MHD-driven kinetic dissipation in the solar wind and corona, *Astrophys. J.* **537**, 1054 (2000).
- [24] G. G. Howes, S. C. Cowley, W. Dorland, G. W. Hammett, E. Quataert, and A. A. Schekochihin, A model of turbulence in magnetized plasmas: Implications for the dissipation range in the solar wind, *J. Geophys. Res. Space Phys.* **113**, A05103 (2008).
- [25] T. H. Thomas, *Waves in Plasmas* (1992), <https://ui.adsabs.harvard.edu/abs/1992wapl.book.....S>.
- [26] Joseph V. Hollweg and Walter Johnson, Transition region, corona, and solar wind in coronal holes: Some two-fluid models, *J. Geophys. Res.* **93**, 9547 (1988).
- [27] C. Y. Tu and E. Marsch, Two-fluid model for heating of the solar corona and acceleration of the solar wind by high-frequency Alfvén waves, *Sol. Phys.* **171**, 363 (1997).
- [28] Steven R. Cranmer, Ion cyclotron wave dissipation in the solar corona: The summed effect of more than 2000 ion species, *Astrophys. J.* **532**, 1197 (2000).
- [29] Joseph V. Hollweg and Philip A. Isenberg, Generation of the fast solar wind: A review with emphasis on the resonant cyclotron interaction, *J. Geophys. Res. Space Phys.* **107**, 1147 (2002).
- [30] Steven R. Cranmer, Ensemble simulations of proton heating in the solar wind via turbulence and ion cyclotron resonance, *Astrophys. J. Suppl. Ser.* **213**, 16 (2014).
- [31] J. L. Kohl *et al.*, First results from the SOHO ultraviolet coronagraph spectrometer, *Sol. Phys.* **175**, 613 (1997).
- [32] J. L. Kohl *et al.*, UVCS/SOHO empirical determinations of anisotropic velocity distributions in the solar corona, *Astrophys. J. Lett.* **501**, L127 (1998).
- [33] Steven R. Cranmer, George B. Field, and John L. Kohl, Spectroscopic constraints on models of ion cyclotron resonance heating in the polar solar corona and high-speed solar wind, *Astrophys. J.* **518**, 937 (1999).
- [34] Lan K. Jian, Christopher T. Russell, Janet G. Luhmann, Robert J. Strangeway, Jared S. Leisner, and Antoinette B. Galvin, Ion cyclotron waves in the solar wind observed by STEREO near 1 AU, *Astrophys. J. Lett.* **701**, L105 (2009).
- [35] J. J. Podesta and S. P. Gary, Magnetic helicity spectrum of solar wind fluctuations as a function of the angle with respect to the local mean magnetic field, *Astrophys. J.* **734**, 15 (2011).
- [36] Jiansen He, Eckart Marsch, Chuanyi Tu, Shuo Yao, and Hui Tian, Possible evidence of Alfvén-cyclotron waves in the angle distribution of magnetic helicity of solar wind turbulence, *Astrophys. J.* **731**, 85 (2011).
- [37] R. T. Wicks, R. L. Alexander, M. Stevens, L. B. Wilson, III, P. S. Moya, A. Viñas, L. K. Jian, D. A. Roberts, S. O’Modhrain, J. A. Gilbert, and T. H. Zurbuchen, A proton-cyclotron wave storm generated by unstable proton distribution functions in the solar wind, *Astrophys. J.* **819**, 6 (2016).
- [38] Lloyd D. Woodham, Robert T. Wicks, Daniel Verscharen, Christopher J. Owen, Bennett A. Maruca, and Benjamin L. Alterman, Parallel-propagating fluctuations at proton-kinetic

- scales in the solar wind are dominated by kinetic instabilities, *Astrophys. J. Lett.* **884**, L53 (2019).
- [39] S. D. Bale, S. T. Badman, J. W. Bonnell, T. A. Bowen, D. Burgess, A. W. Case, C. A. Cattell, B. D. G. Chandran, C. C. Chaston, C. H. K. Chen *et al.*, Highly structured slow solar wind emerging from an equatorial coronal hole, *Nature (London)* **576**, 237 (2019).
- [40] Trevor A. Bowen *et al.*, Ion-scale electromagnetic waves in the inner heliosphere, *Astrophys. J. Suppl. Ser.* **246**, 66 (2020).
- [41] Philip A. Isenberg, Investigations of a turbulence-driven solar wind model, *J. Geophys. Res.* **95**, 6437 (1990).
- [42] Lloyd D. Woodham, Robert T. Wicks, Daniel Verscharen, and Christopher J. Owen, The role of proton cyclotron resonance as a dissipation mechanism in solar wind turbulence: A statistical study at ion-kinetic scales, *Astrophys. J.* **856**, 49 (2018).
- [43] C. F. Kennel and F. Engelmann, Velocity space diffusion from weak plasma turbulence in a magnetic field, *Phys. Fluids* **9**, 2377 (1966).
- [44] Philip A. Isenberg and Martin A. Lee, A dispersive analysis of bispherical pickup ion distributions, *J. Geophys. Res.* **101**, 11055 (1996).
- [45] Philip A. Isenberg, The kinetic shell model of coronal heating and acceleration by ion cyclotron waves: 2. Inward and outward propagating waves, *J. Geophys. Res.* **106**, 29249 (2001).
- [46] E. Marsch and C. Y. Tu, Evidence for pitch angle diffusion of solar wind protons in resonance with cyclotron waves, *J. Geophys. Res.* **106**, 8357 (2001).
- [47] E. Marsch and S. Bourouaine, Velocity-space diffusion of solar wind protons in oblique waves and weak turbulence, *Ann. Geophys.* **29**, 2089 (2011).
- [48] Jiansen He, Linghua Wang, Chuanyi Tu, Eckart Marsch, and Qiugang Zong, Evidence of Landau and cyclotron resonance between protons and kinetic waves in solar wind turbulence, *Astrophys. J.* **800**, L31 (2015).
- [49] S. Peter Gary, Ruth M. Skoug, John T. Steinberg, and Charles W. Smith, Proton temperature anisotropy constraint in the solar wind: ACE observations, *Geophys. Res. Lett.* **28**, 2759 (2001).
- [50] S. Peter Gary, Lan K. Jian, Thomas W. Broiles, Michael L. Stevens, John J. Podesta, and Justin C. Kasper, Ion-driven instabilities in the solar wind: Wind observations of 19 March 2005, *J. Geophys. Res. Space Phys.* **121**, 30 (2016).
- [51] J. C. Kasper, A. J. Lazarus, and S. P. Gary, Hot Solar-Wind Helium: Direct Evidence for Local Heating by Alfvén-Cyclotron Dissipation, *Phys. Rev. Lett.* **101**, 261103 (2008).
- [52] Daniele Telloni, Francesco Carbone, Roberto Bruno, Gary P. Zank, Luca Sorriso-Valvo, and Salvatore Mancuso, Ion cyclotron waves in field-aligned solar wind turbulence, *Astrophys. J. Lett.* **885**, L5 (2019).
- [53] D. Vech *et al.*, Wave-particle energy transfer directly observed in an ion cyclotron wave, *Astron. Astrophys.* **650**, A10 (2021).
- [54] N. J. Fox, M. C. Velli, S. D. Bale, R. Decker, A. Driesman, R. A. Howard, J. C. Kasper, J. Kinnison, M. Kusterer, D. Lario, M. K. Lockwood, D. J. McComas, N. E. Raouafi, and A. Szabo, The solar probe plus mission: Humanity's first visit to our star, *Space Sci. Rev.* **204**, 7 (2016).
- [55] S. D. Bale *et al.*, The FIELDS instrument suite for solar probe plus. Measuring the coronal plasma and magnetic field, plasma waves and turbulence, and radio signatures of solar transients, *Space Sci. Rev.* **204**, 49 (2016).
- [56] Justin C. Kasper *et al.*, Solar wind electrons alphas and protons (SWEAP) investigation: Design of the solar wind and coronal plasma instrument suite for solar probe plus, *Space Sci. Rev.* **204**, 131 (2016).
- [57] J. L. Verniero *et al.*, Parker Solar Probe observations of proton beams simultaneous with ion-scale waves, *Astrophys. J. Suppl. Ser.* **248**, 5 (2020).
- [58] K. G. Klein, J. L. Verniero, B. Alterman, S. Bale, A. Case, J. C. Kasper, K. Korreck, D. Larson, E. Lichko, R. Livi, M. McManus, M. Martinović, A. Rahmati, M. Stevens, and P. Whittlesey, Inferred linear stability of Parker Solar Probe observations using one- and two-component proton distributions, *Astrophys. J.* **909**, 7 (2021).
- [59] J. L. Verniero, B. D. G. Chandran, D. E. Larson, K. Paulson, B. L. Alterman, S. Badman, S. D. Bale, J. W. Bonnell, T. A. Bowen, T. Dudok de Wit, J. C. Kasper, K. G. Klein, E. Lichko, R. Livi, M. D. McManus, A. Rahmati, D. Verscharen, J. Walters, and P. L. Whittlesey, Strong perpendicular velocity-space diffusion in proton beams observed by Parker Solar Probe, *Astrophys. J.* **924**, 112 (2022).
- [60] T. A. Bowen *et al.*, A merged search-coil and fluxgate magnetometer data product for Parker Solar Probe fields, *J. Geophys. Res.* **125**, e2020JA027813 (2020).
- [61] T. Dudok de Wit, V. V. Krasnoselskikh, O. Agapitov, C. Froment, A. Larosa, S. D. Bale, T. Bowen, K. Goetz, P. Harvey, G. Jannet, M. Kretschmar, R. J. MacDowall, D. Malaspina, P. Martin, B. Page, M. Pulupa, and C. Revillet, First results from the SCM search-coil magnetometer on Parker Solar Probe, *J. Geophys. Res. Space Phys.* **127**, e30018 (2022).
- [62] M. Pulupa, S. D. Bale, J. W. Bonnell, T. A. Bowen, N. Carruth, K. Goetz, D. Gordon, P. R. Harvey, M. Maksimovic, J. C. Martínez-Oliveros, M. Moncuquet, P. Saint-Hilaire, D. Seitz, and D. Sundkvist, The Solar Probe Plus Radio Frequency Spectrometer: Measurement requirements, analog design, and digital signal processing, *J. Geophys. Res. Space Phys.* **122**, 2836 (2017).
- [63] F. Sahraoui, M. L. Goldstein, P. Robert, and Yu. V. Khotyaintsev, Evidence of a Cascade and Dissipation of Solar-Wind Turbulence at the Electron Gyroscale, *Phys. Rev. Lett.* **102**, 231102 (2009).
- [64] K. H. Kiyani, S. C. Chapman, Yu. V. Khotyaintsev, M. W. Dunlop, and F. Sahraoui, Global Scale-Invariant Dissipation in Collisionless Plasma Turbulence, *Phys. Rev. Lett.* **103**, 075006 (2009).
- [65] Trevor A. Bowen *et al.*, Constraining Ion-Scale Heating and Spectral Energy Transfer in Observations of Plasma Turbulence, *Phys. Rev. Lett.* **125**, 025102 (2020).
- [66] Christopher Torrence and Gilbert P. Compo, A practical guide to wavelet analysis, *Bull. Am. Meteorol. Soc.* **79**, 61 (1998).
- [67] G. G. Howes and E. Quataert, On the interpretation of magnetic helicity signatures in the dissipation range of solar wind turbulence, *Astrophys. J. Lett.* **709**, L49 (2010).
- [68] Kristopher G. Klein, Gregory G. Howes, Jason M. TenBarge, and John J. Podesta, Physical interpretation of the angle-dependent magnetic helicity spectrum in the solar

- wind: The nature of turbulent fluctuations near the proton gyroradius scale, *Astrophys. J.* **785**, 138 (2014).
- [69] Trevor A. Bowen, Stuart D. Bale, J. W. Bonnell, Davin Larson, Alfred Mallet, Michael D. McManus, Forrest S. Mozer, Marc Pulupa, Ivan Y. Vasko, and J. L. Verniero (PSP/FIELDS and PSP/SWEAP Teams), The electromagnetic signature of outward propagating ion-scale waves, *Astrophys. J.* **899**, 74 (2020).
- [70] R. W. Fredricks and F. V. Coroniti, Ambiguities in the deduction of rest frame fluctuation spectrums from spectrums computed in moving frames, *J. Geophys. Res.* **81**, 5591 (1976).
- [71] Timothy S. Horbury, Miriam Forman, and Sean Oughton, Anisotropic Scaling of Magnetohydrodynamic Turbulence, *Phys. Rev. Lett.* **101**, 175005 (2008).
- [72] T. S. Horbury, R. T. Wicks, and C. H. K. Chen, Anisotropy in space plasma turbulence: Solar wind observations, *Space Sci. Rev.* **172**, 325 (2012).
- [73] C. T. Dum, E. Marsch, and W. Pilipp, Determination of wave growth from measured distribution functions and transport theory, *J. Plasma Phys.* **23**, 91 (1980).
- [74] Adolfo F. Viñas and Chris Gurgiolo, Spherical harmonic analysis of particle velocity distribution function: Comparison of moments and anisotropies using cluster data, *J. Geophys. Res. Space Phys.* **114**, A01105 (2009).
- [75] S. Servidio, A. Chasapis, W. H. Matthaeus, D. Perrone, F. Valentini, T. N. Parashar, P. Veltri, D. Gershman, C. T. Russell, B. Giles, S. A. Fuselier, T. D. Phan, and J. Burch, Magnetospheric Multiscale Observation of Plasma Velocity-Space Cascade: Hermite Representation and Theory, *Phys. Rev. Lett.* **119**, 205101 (2017).
- [76] Joseph T. Parker and Paul J. Dellar, Fourier-Hermite spectral representation for the Vlasov-Poisson system in the weakly collisional limit, *J. Plasma Phys.* **81**, 305810203 (2015).
- [77] A. A. Schekochihin, J. T. Parker, E. G. Highcock, P. J. Dellar, W. Dorland, and G. W. Hammett, Phase mixing versus nonlinear advection in drift-kinetic plasma turbulence, *J. Plasma Phys.* **82**, 905820212 (2016).
- [78] J. Squire, B. D. G. Chandran, and R. Meyrand, In-situ switchback formation in the expanding solar wind, *Astrophys. J. Lett.* **891**, L2 (2020).
- [79] Benjamin D. G. Chandran and Jean C. Perez, Reflection-driven magnetohydrodynamic turbulence in the solar atmosphere and solar wind, *J. Plasma Phys.* **85**, 905850409 (2019).
- [80] Petr Hellinger, Pavel M. Trávníček, Štěpán Štverák, Lorenzo Matteini, and Marco Velli, Proton thermal energetics in the solar wind: Helios reloaded, *J. Geophys. Res. (Space Phys.)* **118**, 1351 (2013).
- [81] K. Sasikumar Raja, Prasad Subramanian, Madhusudan Ingale, R. Ramesh, and Milan Maksimovic, Turbulent proton heating rate in the solar wind from 5-45  $R_{\odot}$ , *Astrophys. J.* **914**, 137 (2021).
- [82] H. Politano and A. Pouquet, von Kármán-Howarth equation for magnetohydrodynamics and its consequences on third-order longitudinal structure and correlation functions, *Phys. Rev. E* **57**, R21 (1998).
- [83] Riddhi Bandyopadhyay *et al.*, Enhanced energy transfer rate in solar wind turbulence observed near the sun from Parker Solar Probe, *Astrophys. J. Suppl. Ser.* **246**, 48 (2020).
- [84] N. Andrés, F. Sahraoui, S. Huang, L. Z. Hadid, and S. Galtier, The incompressible energy cascade rate in anisotropic solar wind turbulence, *Astron. Astrophys.* **661**, A116 (2022).
- [85] Joshua E. Stawarz, Charles W. Smith, Bernard J. Vasquez, Miriam A. Forman, and Benjamin T. MacBride, The turbulent cascade and proton heating in the solar wind at 1 AU, *Astrophys. J.* **697**, 1119 (2009).
- [86] K. T. Osman, M. Wan, W. H. Matthaeus, J. M. Weygand, and S. Dasso, Anisotropic Third-Moment Estimates of the Energy Cascade in Solar Wind Turbulence Using Multi-spacecraft Data, *Phys. Rev. Lett.* **107**, 165001 (2011).
- [87] Benjamin D. G. Chandran, Bo Li, Barrett N. Rogers, Eliot Quataert, and Kai Germaschewski, Perpendicular ion heating by low-frequency Alfvén-wave turbulence in the solar wind, *Astrophys. J.* **720**, 503 (2010).
- [88] Jonathan Squire, Romain Meyrand, Matthew W. Kunz, Lev Arzamasskiy, Alexander A. Schekochihin, and Eliot Quataert, High-frequency heating of the solar wind triggered by low-frequency turbulence, *Nat. Astron.* **6**, 715 (2022).
- [89] Daniel Verscharen, Sofiane Bourouaine, and Benjamin D. G. Chandran, Instabilities driven by the drift and temperature anisotropy of alpha particles in the solar wind, *Astrophys. J.* **773**, 163 (2013).
- [90] J. V. Shebalin, W. H. Matthaeus, and D. Montgomery, Anisotropy in MHD turbulence due to a mean magnetic field, *J. Plasma Phys.* **29**, 525 (1983).
- [91] P. Goldreich and S. Sridhar, Toward a theory of interstellar turbulence. II. Strong Alfvénic turbulence, *Astrophys. J.* **438**, 763 (1995).
- [92] R. Meyrand, J. Squire, A. A. Schekochihin, and W. Dorland, On the violation of the zeroth law of turbulence in space plasmas, *J. Plasma Phys.* **87**, 535870301 (2021).
- [93] Joshua E. Stawarz, Charles W. Smith, Bernard J. Vasquez, Miriam A. Forman, and Benjamin T. MacBride, The turbulent cascade for high cross-helicity states at 1 AU, *Astrophys. J.* **713**, 920 (2010).
- [94] C. H. K. Chen *et al.*, The evolution and role of solar wind turbulence in the inner heliosphere, *Astrophys. J. Suppl. Ser.* **246**, 53 (2020).
- [95] Die Duan *et al.*, The radial dependence of proton-scale magnetic spectral break in slow solar wind during PSP encounter 2, *Astrophys. J. Suppl. Ser.* **246**, 55 (2020).
- [96] Die D, Jansen He, Trevor A. Bowen, Lloyd D. Woodham, Tieyan Wang, Christopher H. K. Chen, Alfred Mallet, and Stuart D. Bale, Anisotropy of solar wind turbulence in the inner heliosphere at kinetic scales: PSP observations, *Astrophys. J. Lett.* **915**, L8 (2021).
- [97] F. S. Mozer, O. V. Agapitov, S. D. Bale, J. W. Bonnell, T. A. Bowen, and I. Vasko, DC and low-frequency electric field measurements on the Parker Solar Probe, *J. Geophys. Res. Space Phys.* **125**, e27980 (2020).
- [98] Michael D. McManus *et al.*, Cross helicity reversals in magnetic switchbacks, *Astrophys. J. Suppl. Ser.* **246**, 67 (2020).